Catalytic Distillation in Structured Packings: Methyl Acetate Synthesis

Andrzej Górak
Dept. of Chemical Engineering, University of Dortmund, 44221 Dortmund, Germany

Achim Hoffmann
Dept. of Mechanical Engineering, University of Essen, 45117 Essen, Germany

Catalytic Distillation can improve process design, the design of column internals requires special attention. The catalytic packing MULTIPAK facilitates effective catalysis, high separation efficiency, and a wide loading range simultaneously. In this work the main characteristics of MULTIPAK — pressure drop, loading range, and separation efficiency — are determined experimentally. The developed nonequilibrium stage model developed reflects the complexity of catalytic distillation processes and comprises correlations describing pressure drop and separation efficiency of MULTIPAK as a function of the operating conditions. The model has been implemented in the simulation environment Aspen Custom Modeler, and the simulation results are compared with experimental data for the synthesis of methyl acetate. This model reflects the process behavior, but differences between simulated results and experimental data can still be observed.

Introduction

The combination of heterogeneously catalyzed reaction and separation in one single process unit, known as catalytic distillation, offers new potential for improved process design. Even if not a new concept, it still bears a lot of advantages compared to the conventional approach where reaction and separation are carried out sequentially. One of those advantages is the elimination of equipment for product recovery and recycling of unconverted reactants, which leads to savings in capital and operation costs. Catalytic distillation may also improve selectivity, mass transfer and process control, and avoid catalyst fouling. On the other hand, the installation of a solid catalyst in a distillation column conflicts with these benefits since it complicates the design of catalytic distillation processes.

One of the major problems is the choice of suitable catalytic column internals. Those devices have to reconcile satisfactory separation efficiency and catalytic activity without limiting possible column loads. Catalyst bales, covering a large percentage of the column cross section, have been used successfully in commercial-scale MTBE production, but high-capacity devices can lower capital costs for catalytic distillation columns (Fair, 1998). However, designing a catalytic distillation column requires knowledge of device characteristics, as well as of reaction kinetics, and chemical and vapor-liquid equilibrium. A suitable model is indispensable to reflect the complex behavior of catalytic distillation columns. In recent years, great effort has been made to investigate the relevant phenomena occurring in catalytic distillation processes. A detailed overview of different aspects of reactive distillation processes has been given recently by Taylor and Krishna (2000).

The analysis of reactive distillation from a thermodynamic point of view, as done by Ung and Doherty (1995), Nisoli et al. (1997), or Frey and Stichlmair (1999), allows to check if the process is feasible or to identify the presence of reactive azeotropes and attainable regions for product compositions. Okansinski and Doherty (1997) outlined the important role of uncertainties in model parameters at this early stage of designing reactive distillation columns. They become even more important when the steady-state and dynamic behavior of a reactive distillation column should be predicted. Models of different complexity have been presented to describe the behavior of catalytic distillation processes. Bessling et al. (1998) analyzed the process of methyl acetate synthesis via catalytic distillation using a simple model assuming chemical

Correspondence concerning this article should be addressed to .

and vapor-liquid equilibrium on all stages. A steady-state rate-based model for the production of diacetone alcohol with catalytic distillation was developed by Podrebarac et al. (1998b). Higler et al. (1999) and Kenig et al. (1999) presented a nonequilibrium model for reactive distillation columns using the Maxwell-Stefan equations to describe mass transfer between the vapor and liquid phase. Sundmacher and Hoffmann (1996) proposed a detailed nonequilibrium model including the mass-transfer resistance between the liquid phase and the porous catalyst for the MTBE process. Bart and Landschützer (1996) analyzed the influence of axial dispersion and varying model parameters on the performance of catalytic distillation columns. Schneider et al. (1999) developed a dynamic model for the production of methyl-acetate using reactive batch distillation. A comparison between equilibrium and nonequilibrium models by Lee and Dudukovic (1998) for reactive distillation columns for the production of ethyl-acetate showed that the reaction rate is the main factor that affects the column behavior, a fact that was also pointed out by Podrebarac et al. (1998a). Subwalla and Fair (1999) used an equilibrium stage model to derive design guidelines for catalytic distillation systems considering several key design parameters such as pressure, reactive zone location, reactant feed ratio, feed location, amount of catalyst, column diameter, and the number of equilibrium stages in reactive and nonreactive zones, but they recommend the use of a rate-based model to determine the height of the column.

Extensive experimental work has been performed to investigate the behavior of reactive column internals. The hydrodynamics of catalyst bales used for MTBE production have been determined by Zheng and Xu (1992), Xu et al. (1997) and Subwalla et al. (1997), while Huang et al. (1998) investigated the mass-transfer behavior of a laboratory-scale packing for the aldol condensation. Recently, several investigations concerning the hydrodynamic behavior of the catalytic packing Katapak-S have been presented by Moritz et al. (1999), Moritz and Hasse (1999), as well as Ellenberger and Krishna (1999). Since the reaction kinetics has been recognized as a model-parameter of great influence, it has been determined experimentally for different catalytic distillation processes. The synthesis of methyl acetate mentioned in this study has been investigated by Xu and Chuang (1996, 1997) and Pöpken et al. (1999, 2000).

This article presents a concept for the design of catalytic distillation processes with the catalytic packing MULTIPAK, based on a nonequilibrium model. All model parameters needed for this approach have been derived from experiments, independent of the catalytic distillation process.

Structured Catalytic Packing

The catalytic packing MULTIPAK (DE 197 01 045 A1, 1997) has been developed in consideration of the qualities of modern structured wire gauze packings and their improvements on conventional distillation. MULTIPAK is manufactured by Julius Montz GmbH. It consists of corrugated wire gauze sheets (1) and catalyst bags of the same material (2) assembled in alternate sequence, as shown in Figure 1. This construction enables high column loads by providing open channels for the gas flow, while most of the liquid is flowing downwards through the catalyst bags. Sufficient mass transfer between the gas and liquid phase and radial mixing is guaranteed by the segmentation of the catalyst bags and numerous contact spots with the wire gauze sheets. The catalyst bags can be filled with different types of particle shape catalyst, and in case of the methyl acetate synthesis, an acidic ion exchange resin (Lewatit K2621, Bayer AG) was used. The applicability of MULTIPAK in catalytic distillation has already been proven by a series of catalytic batch distillation experiments with the methyl acetate synthesis chosen as an example process (Kreul et al., 1998; Schneider et al., 1999).

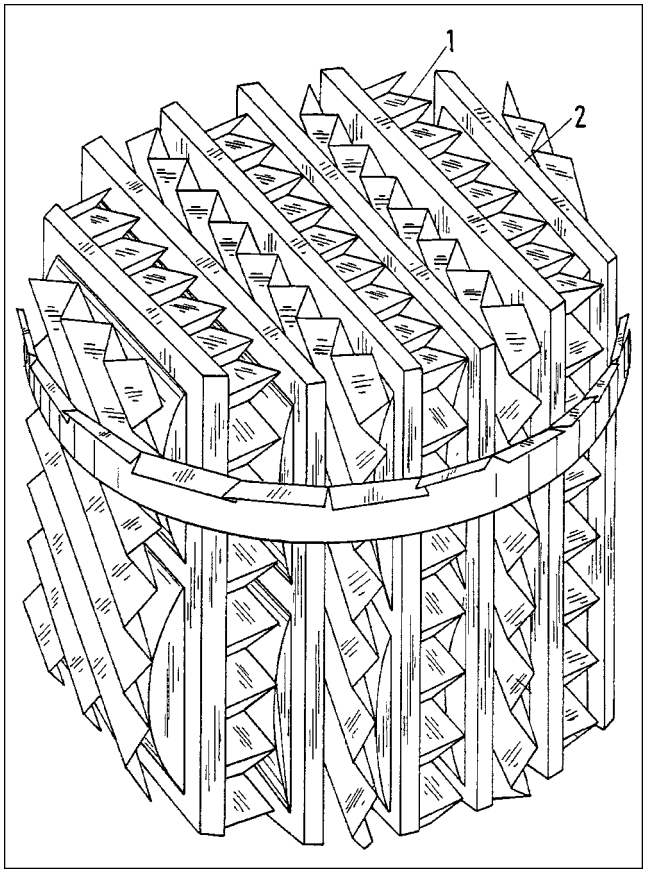

Figure 1. Construction of MULTIPAK.

Two different types of MULTIPAK can be distinguished. The layers of corrugated wire gauze sheets of MULTIPAK-I have an inclination angle of 60 degrees and a specific surface area of 500 m^2/m^3, while MULTIPAK-II comprises sheets with an inclination of 45 degrees and a specific surface area of 750 m^2/m^3. Catalyst bags used for MULTIPAK-II are thicker than for MULTIPAK-I and allow a higher catalyst volume fraction in combination with a reduced specific surface area. Therefore, specific requirements of the process can be taken into account with the choice of the packing type. To ensure a similar hydrodynamic behavior of laboratory- and technical-scale packings, both consist of the same elements. However, weld joints at the edges of the catalyst bags and the gap between the packing and the column wall result in less catalyst volume fraction, less specific surface area, and a higher void fraction for laboratory-scale packings. This has to

Table 1. Characteristic Geometrical Data of the Investigated Packings

	A	B
Type of packing	MULTIPAK-I	MULTIPAK-II
Column dia., d [mm]	98	52
Hgt. of packing segment H_P [mm]	166	166
Catalyst vol. faction ψ_{Cat}	0,250	0,336
Specific surface area a [m^2/m^3]	370	270
Void fraction ϵ	0,643	0,580
Inclination angle θ [deg]	60	45
Corrugation spacing S [mm]	7,5	5,6

be considered for the scale-up of reactive distillation processes with MULTIPAK. The characteristic geometrical data of the two different laboratory-scale packings which were investigated in this study are listed in Table 1.

Packing Characteristics

In order to determine the pressure drop and loading range of MULTIPAK, experiments were performed for both packing types. They have been carried out in glass columns with a total packing height of 1 m at ambient pressure. Air/water has been used as a test system with a circulating liquid phase set at a constant temperature of 20°C. Liquid and gas flow was measured with calibrated rotameters. To ensure a complete wetting of the catalytic packing, the column was operated at maximum liquid loads before setting the desired gas and liquid flow. When steady-state conditions were reached, the pressure drop over the packed section of the column was measured. The results of these experiments are shown in Figures 2a and 2b, where the specific pressure drop of MULTIPAK is plotted vs. the gas load for different liquid loads. To ensure a comparability with the process conditions in distillation columns, the F-Factor

$$F = u_{Gs} \cdot \sqrt{\rho_G} \tag{1}$$

was used for the gas load and the superficial liquid velocity for the liquid load. Each dot represents an experimental point,

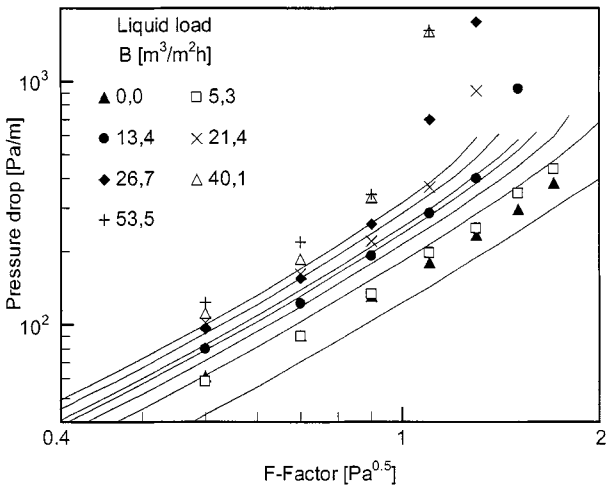

Figure 2a. Pressure drop of packing A.

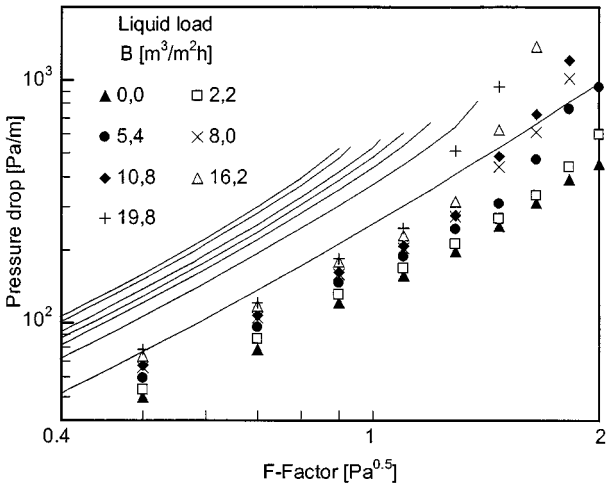

Figure 2b. Pressure drop of packing B.

while the straight lines have been derived by applying the hydraulic model by Rocha et al. (1993) to MULTIPAK.

The experimental data covers a wide range of possible column loads in both cases, even if the gas load for packing A was restricted to an F-Factor of 1.7 Pa$^{0.5}$ due to limitations of the experimental setup. Therefore, flooding of packing A was only observed at higher liquid loads. Two different flow regimes similar to those of conventional structured packings can be observed. At column loads below the loading point, the slope of the pressure drop vs. gas load remains the same as for the dry packing. A further increase of the gas flow results in a steeper slope, since the liquid is dammed up by the gas flow and reduces the hydraulic diameter of the open channels for the gas flow. Flooding of the packing can be observed at pressure drop above 10^3 Pa/m. The feasible column loads for MULTIPAK are very similar to those reported by Moritz and Hasse (1999) for Katapak-S.

A comparison of the experimental data with a mechanistically-based model for structured packings (Rocha et al., 1993) shows inconsistent results for the two packings. While the pressure drop of packing A below the loading point can be described with an accuracy of 30%, the pressure drop predicted for packing B is about two times higher than the experimental values. This can be caused by the wall effects in small diameter columns. The weld joints at the edges of the catalyst bags provide vertical channels for the gas flow and therefore enable a bypass with reduced flow resistance. The only modification to the original model has been made in assuming a total wetting of the packing surface, due to the excellent wettability of the wire gauze material used for MULTIPAK. The hydraulic model of Rocha et al. (1993) seems to be a suitable option to predict the pressure drop of MULTIPAK in a bigger than laboratory scale. A statement that has to be proven by further experiments with technical-scale packings.

Apart from pressure drop and loading range, the separation efficiency of the packing plays an important role in the design of catalytic distillation columns. Therefore, distillation experiments have been carried out with the test system chlorobenzene/ethylbenzene, which has been recommended by Onken and Arlt (1990) as a mixture for testing column

internals at atmospheric pressure or vacuum. The distillation column was equipped with 2 m of the catalytic packing A and operated with total reflux. The column load was changed by varying the heat duty and the operating pressure from 10 to 60 kPa, to cover the whole loading range of the packing. When steady-state conditions were reached, liquid samples were taken directly above and below the catalytic packing and analyzed via gas chromatography. The separation efficiency characterized by the number of theoretical stages can be calculated from the Fenske-equation (Stichlmair and Fair, 1998)

$$n_{th} = \frac{1}{\ln \alpha} \cdot \ln\left(\frac{x_D}{x_B} \cdot \frac{1 - x_B}{1 - x_D}\right) \tag{2}$$

The application of Eq. 2 is limited to ideal binary systems; for the used test system this requirement is only fulfilled for operating pressures above 40 kPa. However, for lower operating pressures, the deviation from a mean relative volatility $\bar{\alpha}$ is below 0.2% (Onken and Arlt, 1990). Equation 2 is therefore used for all operating pressures with a mean relative volatility calculated by

$$\bar{\alpha} = \exp \int_{x_B}^{x_D} \ln \alpha(x)\, dx. \tag{3}$$

The number of theoretical stages per meter of the catalytic packing NTSM is given by

$$\text{NTSM} = \frac{n_{th}}{H}. \tag{4}$$

Figure 3 shows the *NTSM*-value of packing A as a function of the column load, given by the F-Factor. For the whole range of column loads, the separation efficiency is at least four theoretical stages per meter. It remains constant for a wide loading range of the packing, but increases up to *NTSM* = 6 for lower column loads. This phenomenon was already reported by Pelkonen et al. (1997) for the conventional structure packing Montzpak A3-500 whose corrugated wire gauze sheets are identical with MULTIPAK-I. Moritz and Hasse (1999) determined a value of *NTSM* = 3 for the laboratory-scale KATAPAK-S.

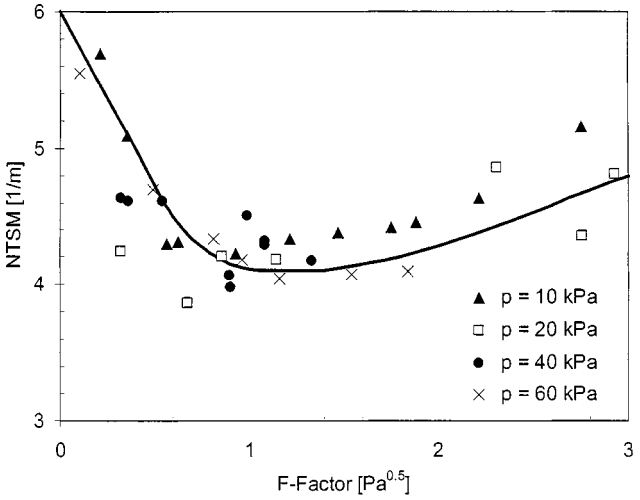

Figure 3. Separation efficiency of packing A.

To enable the use of a nonequilibrium stage model for the design of reactive distillation columns equipped with MULTIPAK, mass-transfer coefficients and their dependence on column loads have to be available. They can be determined from the total reflux distillation experiments described above. Following the concept of transfer units (Chilton and Colburn, 1935), an overall mass-transfer coefficient can be calculated from

$$k_{OG} = \frac{4\dot{L}}{\pi c_{t,G} d^2 a H}\left[\frac{1}{\alpha - 1}\ln\left(\frac{x_D}{x_B} \cdot \frac{1 - x_B}{1 - x_D}\right) + \ln\left(\frac{1 - x_B}{1 - x_D}\right)\right]. \tag{5}$$

According to the generally adopted two-film theory, the relationship between the overall height of the gas phase transfer unit HTU_{OG} and the individual film transfer units HTU_G and HTU_L is given by

$$\text{HTU}_{OG} = \text{HTU}_G + m\,\text{HTU}_L. \tag{6}$$

Even if the mass-transfer resistance in the liquid phase is almost negligible in most distillation applications (Olujic et al., 1999), the penetration approach is widely used to calculate the liquid phase mass-transfer coefficient. It can be calculated from

$$\beta_L = 2\sqrt{\frac{0.9 D_L u_{L,\text{eff}}}{\pi S}} \tag{7}$$

(Rocha et al., 1996) with the effective liquid velocity defined as

$$u_{L,\text{eff}} = \frac{u_{L,s}}{\epsilon h_L \sin\theta}. \tag{8}$$

The liquid holdup h_L was calculated according to the hydraulic model for structured packings presented by Rocha et al. (1993). Assuming that this approach is also suitable for the catalytic packing due to the similar geometry of the gas-liquid flow channels, the vapor-phase mass-transfer coefficient can be calculated from

$$\beta_G = \frac{k_{OG}}{1 - m\dfrac{k_{OG} u_{L,s}}{\beta_L u_{G,s}}}. \tag{9}$$

The experimental values of vapor-phase mass-transfer coefficients have been correlated in the well known form of dimensionless groups. The following correlation

$$Sh_G = 0.0064\, Re_G^{0.96} Sc_G^{0.33}. \tag{10}$$

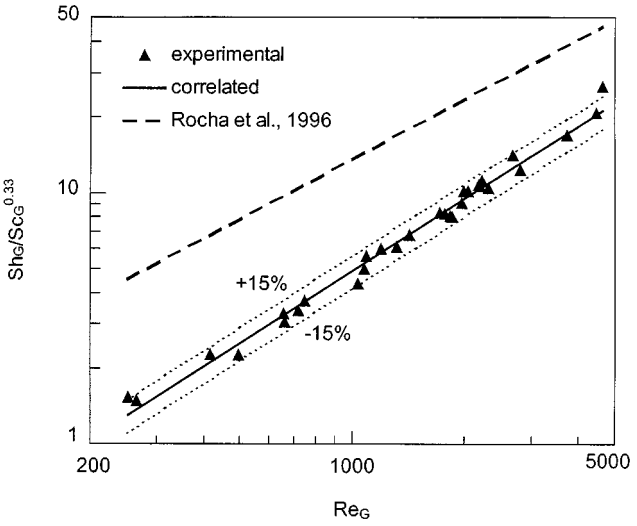

Figure 4. Vapor-phase mass-transfer coefficients.

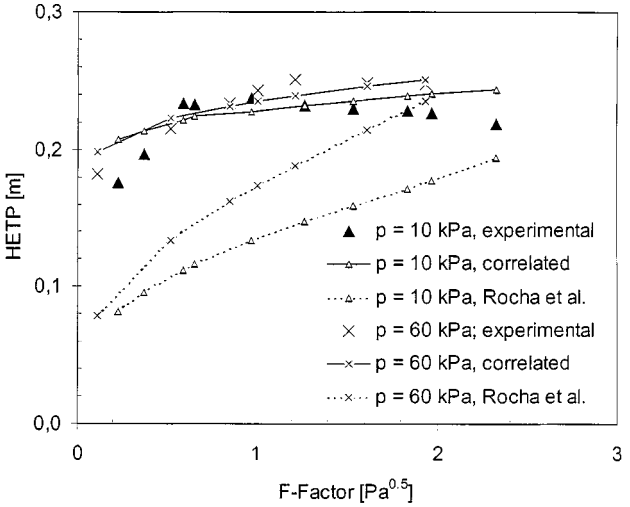

Figure 5. HETP values for packing A.

reproduces all experimental data within an accuracy of 15%, as shown in Figure 4. The dimensionless groups have been defined according to Rocha et al. (1996) with

$$u_{G,\text{eff}} = \frac{u_{G,s}}{\epsilon(1-h_L)\sin\theta}. \tag{11}$$

A comparison with mass-transfer coefficients calculated from the correlation of Rocha et al. (1996) shows that these values are considerably higher than the experimental values. This has already been noted by Olujic et al. (1999) who explained the significant difference with the unrealistic effective surface area proposed by Rocha et al. (1996). Since we assumed a total wetting of the wire gauze material, the effective surface area is considerably higher. To enable a comparison, HETP (height equivalent of a theoretical plate) values have been calculated with both methods using the equation

$$\text{HETP} = \frac{\ln m}{m-1}\left(\frac{u_{G,s}}{\beta_G a} + \lambda\frac{u_{L,s}}{\beta_L a}\right) \tag{12}$$

and compared with the experimental data. The results for two experimental series are shown in Figure 5. It can be seen that the correlation presented here reflects the experimental data within an accuracy of 20%, while the HETP values calculated with the method of Rocha et al. (1996) are considerably lower. Due to the stronger dependency of mass-transfer efficiency on the column load, the maximum deviation occurs at low column loads, while the theoretical curve approaches the experimental values at higher loads.

Pilot-plant experiments

Theoretical and experimental results for the synthesis of methyl acetate via catalytic batch distillation with MULTIPAK have already been presented by Kreul et al. (1998) and Schneider et al. (1999). To evaluate the influence of the packing characteristics on the process, a pilot-plant column as shown in Figure 6 has been built up to investigate experimentally the continuous process behavior. The column design is similar to that presented by Krafczyk and Gmehling (1994) or Bessling et al. (1998) with an inner column diameter of 50 mm and an effective packing height of 4 m meter comprising 4 sections of 1 m each. A reactive section of 2 m is located in the middle of the column with two nonreactive sections of 1 m each below and above. The reactive section is equipped with MULTIPAK-I and the nonreactive section with Montz-Pak A3-500. High conversion can only be achieved if the reactants can flow countercurrently in the reactive section (Agreda et al., 1990); thus, methanol is fed to the column below the reactive section, while the acetic acid feed is located above the catalytic packing. Special attention has been paid to allow for a comparison of experimental and theoretical process data. The flow rates of feed-, product- and reflux-streams are determined via mass-flow measurements to ensure the accurate evaluation of process conditions. Liquid samples can be taken from all streams mentioned above, as well as along the column height. The samples have been analyzed by gas-chromatography to determine the mass-fraction of all organic components and Karl-Fischer titration to ascertain the amount of water. Resistance thermometers have been installed for all inlet and outlet streams and along the column height. This enables together with a heated jacket to prevent heat loss—a factor of great influence in small diameter columns—to draw an exact energy balance of the column. All data is recorded by a process control system and a data-reconciliation ensures that the mass-balance of the column is fulfilled for all experimental runs.

A series of experiments have been performed with a stoichiometric feed ratio of acetic acid and methanol. The process conditions characterized by feed and distillate flow rates and reflux-ratio are listed in Table 2 together with the experimental conversion and the mass fraction of methyl acetate in the distillate stream.

Six experiments have been performed with feed mass flows of 1.4 kg/h and 2.0 kg/h. The reflux ratio has been varied from 1.62 to 2.55 in experiments 1 to 5, while the other operating conditions (feed and distillate mass flow) has been kept

Table 2. Experimental Results

No.	Total Feed Mass-Flow $\dot{m}_F$ [kg/h]	Distillate Mass-Flow $\dot{m}_D$ [kg/h]	Reflux ratio RR	Conv. of Acetic Acid ξ_{exp}	Purity of Distillate w_{exp} [kg/kg]
1	1.39	1.04	1.62	0.761	0.809
2	1.39	1.05	1.99	0.806	0.851
3	1.41	1.06	2.39	0.803	0.827
4	1.41	0.99	2.51	0.806	0.881
5	1.41	1.00	2.55	0.790	0.861
6	2.01	1.65	0.97	0.827	0.782

at constant values. The experimental conversion of acetic acid is well above the equilibrium value of 0.695 in all experiments, but does not reach the high conversions reported for the industrial process (Agreda et al., 1990). Conversion can be improved by increasing the height of the reactive section as reported by Bessling et al. (1998) who compared a pilot-plant reactive distillation column including 13 reactive stages with an industrial column design comprising 38 reactive stages. The reactive section in our experimental setup has only 8 theoretical stages; thus, conversion is considerably lower.

For the same reason, the purity of the distillate stream is low in comparison to the industrial process. Since not all methanol is converted to methyl acetate, it enters the upper rectifying section of the column and is enriched towards the top. However, the objective of the experimental work presented here was not to produce high-purity methyl acetate, but providing experimental data of the process behavior to be compared with theoretical results derived from process simulation.

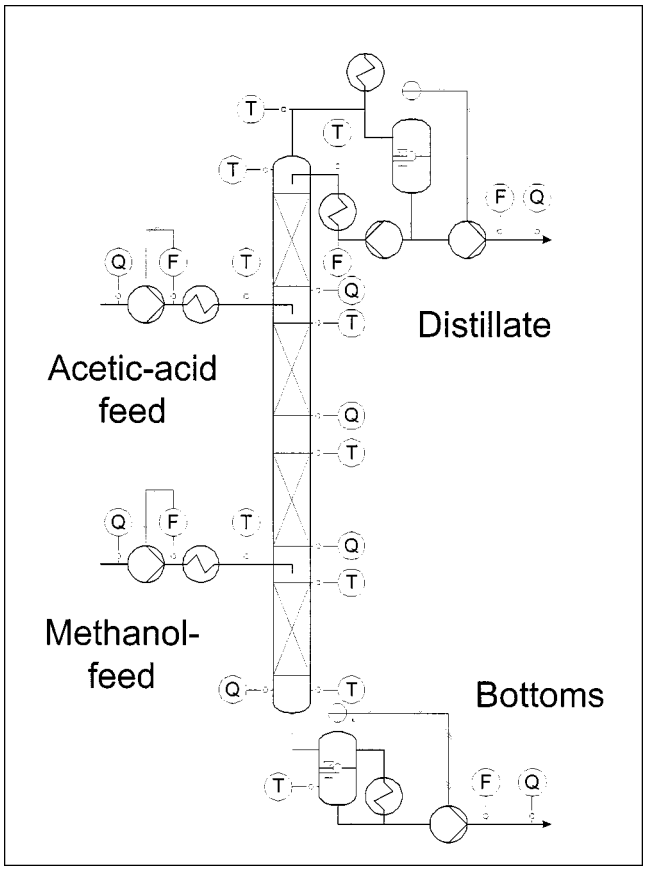

Figure 6. Experimental setup.

Modeling

A rigorous dynamic model for catalytic distillation processes has been presented by Schneider et al. (1999) combining the dynamic balance equations required for batch operation and the rate-based approach for the appropriate description of multicomponent mass transfer. This model has been modified in view of the availability of model parameter for the catalytic packing MULTIPAK and experimental investigation described above. Thus, the time derivatives in the balance equations have been set equal to zero, since only steady-state simulations have been performed and compared with experimental data.

For the nonequilibrium model, the reactive distillation column was subdivided into a number of segments. The model for each segment j is based on the two-film theory (Taylor and Krishna, 1993), and therefore consists of an ideally mixed vapor and liquid bulk phase, as well as two film regions adjacent to the interface as shown in Figure 6. The catalyzed reaction has been considered as quasi-homogeneous with no mass-transfer resistance between liquid phase and catalyst. This assumption has already been described as justified for the synthesis of methyl acetate by several authors (Krafczyk and Gmehling, 1994; Xu and Chuang, 1997). However, sorption effects inside the ion-exchange catalyst should not be neglected (Kreul et al., 1998).

Pöpken et al. (2000) recently published an extensive experimental study on the reaction kinetics and chemical equilibrium of the system methanol/acetic acid//methyl acetate/water. They derived an adsorption-based model for the heterogeneously catalyzed reaction choosing the ion-exchange resin Amberlyst 15 (Rohm and Haas Co.) as catalyst.

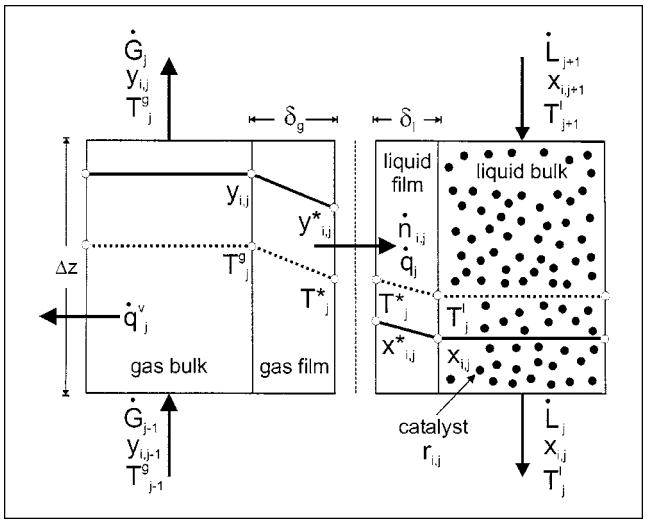

Figure 7. Two-film model for a reactive packing segment.

This model does not only consider thermodynamic nonidealities by using liquid-phase activities for the reaction kinetic and equilibrium equations, but also sorption and swelling effects. The physical properties of Amberlyst 15 are very similar to those of Lewatit K2621 used here. However, the concentration of acid sites for dry Lewatit K2621 has been determined experimentally as 4.55 $\mathrm{mol}^{H+}/g_{Cat}$, close to the value of 4.75 $\mathrm{mol}^{H+}/g_{Cat}$ reported for Amberlyst 15. Therefore, this model was adopted and, for consistency, the UNIQUAC approach was used for vapor-liquid equilibrium with binary interaction parameters also taken from Pöpken et al. (2000).

The component balances for the gas and liquid phase on a non-equilibrium stage j were written as

$$0 = \dot{G}_{j-1} y_{i,j-1} - \dot{G}_j y_{i,j} - \dot{n}_{i,j} a \frac{\pi}{4} d^2 \Delta z \qquad i = 1 \ldots n \quad (13)$$

$$0 = \dot{L}_{j+1} x_{i,j+1} - \dot{L}_j x_{i,j} + \left(\dot{n}_{i,j} a + r_{i,j} \psi_{\mathrm{cat}} \rho_{\mathrm{cat}} \right) \frac{\pi}{4} d^2 \Delta z. \qquad i = 1 \ldots n \quad (14)$$

The component balances are completed with the summation conditions for the mol fractions in both phases

$$\sum_{i=1}^{n} x_{i,j} = \sum_{i=1}^{n} y_{i,j} = 1. \quad (15)$$

The interfacial mass-transfer rates have been calculated with the Maxwell-Stefan approach to account for diffusional interaction and thermodynamic nonidealities. To relate the multicomponent mass-transfer rates to the binary mass-transfer experiments described above, the method of Krishna and Standart (1979) was used. The diffusional fluxes can be calculated from

$$(J) = - c_{t,G}^{\mathrm{av}} [k_G^{\mathrm{av}}] (y_{i,j}^* - y_{i,j}) = - c_{T,L}^{\mathrm{av}} [k_L^{\mathrm{av}}] [\Gamma_L^{\mathrm{av}}] (x_{i,j} - x_{i,j}^*) \quad (16)$$

with the matrix of mass-transfer coefficients defined as

$$[k^{\mathrm{av}}] = [R^{\mathrm{av}}]^{-1} \quad (17)$$

with

$$R_{ii} = \frac{y_i^{\mathrm{av}}}{\kappa_{in}} + \sum_{\substack{k=1 \\ k \neq i}}^{n} \frac{y_k^{\mathrm{av}}}{\kappa_{ik}} \qquad i = 1 \ldots n-1 \quad (18)$$

$$R_{ij} = - y_i^{\mathrm{av}} \left(\frac{1}{\kappa_{ij}} - \frac{1}{\kappa_{in}} \right) \qquad i,j = 1 \ldots n-1 \quad (19)$$

The binary mass-transfer coefficients κ_{ij} can be derived from suitable mass-transfer correlations for binary systems, using the appropriate Maxwell-Stefan diffusion coefficient. For the reactive column section, the mass-transfer correlation for MULTIPAK (Eqs. 7–10) was used. The mass transfer in the nonreactive sections was calculated according to Rocha et al. (1996), using the geometrical characteristics of Montz-Pak A3-500.

The linearized theory of Toor, Stewart, and Prober (Stewart and Prober, 1964) can be applied to evaluate $[R^{\mathrm{av}}]$, $[\Gamma^{\mathrm{av}}]$ and all physical properties, using an average mol-fraction defined as

$$y_{i,j}^{\mathrm{av}} = \frac{y_{i,j}^* + y_{i,j}}{2} \qquad i = 1 \ldots n. \quad (20)$$

Phase equilibrium is assumed at the interface with interfacial compositions calculated from

$$y_{i,j}^* = K_{i,j}^{\mathrm{eq}} x_{i,j}^* \qquad i = 1 \ldots n \quad (24)$$

with vapor-liquid equilibrium constants $K_{i,j}^{\mathrm{eq}}$ determined from the UNIQUAC equations and the extended Antoine equation for vapor pressure (Reid et al., 1987).

Since only n-1 diffusional fluxes are independent, the energy balances for both phases including the conductive heat flux across the interface are formulated to relate the diffusional fluxes to the component molar fluxes (Higler et al., 1999). They are written as follows

$$0 = \dot{G}_{j-1} h_{G,j-1} - \dot{G}_j h_{G,j} - \left(\dot{q}_j^v + \dot{q}_j^* \frac{ad}{4} \right) \pi d \Delta z \qquad i = 1 \ldots n \quad (25)$$

$$0 = \dot{L}_{j+1} h_{L,j+1} - \dot{L}_j h_{L,j} + \dot{q}_j^* \frac{\pi}{4} a d^2 \Delta z \qquad i = 1 \ldots n \quad (26)$$

The heat transfer across the vapor-liquid interface consist of a convective and conductive part and can be calculated from

$$\dot{q}_j^* = - \frac{\lambda_g^{\mathrm{av}}}{\bar{\delta}_G} (T_J^* - T_{G,j}) + \sum_{i=1}^{n} \dot{n}_{i,j} h_{G,i,j} = - \frac{\lambda_l^{\mathrm{av}}}{\bar{\delta}_L} (T_{L,j} - T_j^*) + \sum_{i=1}^{n} \dot{n}_{i,j} h_{G,i,j}. \quad (27)$$

The film thickness in both phases is needed to calculate the conductive interfacial heat transfer, but in multicomponent systems only individual film thicknesses δ_{ij} can be derived from binary mass transfer coefficients.

$$\delta_{ij} = \frac{\mathcal{D}_{ij}}{\kappa_{ij}} \quad (28)$$

Therefore, a mean film thickness has been defined as

$$\bar{\delta} = \frac{1}{n(n-1)} \sum_{i=1}^{n} \sum_{\substack{j=1 \\ j \neq i}}^{n} \delta_{ij} \quad (29)$$

This approximation is justified since all individual film-thickness are similar and the conductive heat transfer across the interface is small in comparison to the convective transfer. It has to be emphasized that the mean film thickness is only

used to calculate the conductive heat transfer and not for the evaluation of individual mass transfer across the interface.

The segmentation of the catalytic distillation column in axial direction together with the detailed rate-based approach results in a complex and highly nonlinear algebraic system of equations. All model equations have been implemented in the commercial simulation environment Aspen Custom Modeler. A first guess of the bulk phase compositions and temperatures was provided by the solution of an equilibrium stage model without reactions as done by Powers et al. (1988). The first convergent initialization of the rate-based approach was achieved by implementing effective diffusion coefficients, which leads to decoupled mass-transfer equations. This simplified model has been extended by adding reaction terms and the Maxwell-Stefan approach.

Results

Theoretical and experimental results for the synthesis of methyl acetate via catalytic batch distillation with MULTIPAK have already been presented by Kreul et al. (1998) and Schneider et al. (1999). To ascertain the influence of packing characteristics on the process behavior, a continuous process is investigated within this work. The main objective was a comparison between theoretical and experimental results to determine the ability of the model to predict the process behavior.

Process simulations have been performed for experiments 1 to 5, as listed in Table 2. The feed was stoichiometric with a total mass flow of 1.4 kg/h, while the distillate flow rate was held constant at 1.04 kg/h. The process conditions were varied by changing the reflux ratio from 0.05 up to 4. Figure 8 shows simulation results for the conversion of acetic acid and the purity of the distillate stream in mass-fraction together with the experimental results (experiments 1 to 5).

The simulation results show a maximum of conversion and purity at a reflux ratio of 1.2 with a strong decrease towards lower reflux ratios. Increasing the reflux ratio beyond the optimum also results in lower conversion and purity, but they remain almost constant for reflux ratios above 2. A similar behavior was already reported by Bessling et al. (1998) for this process, but they determined an optimal reflux ratio of 1.5 and a constant conversion of 0.66 for reflux ratios above 10. Unfortunately, a direct comparison of the results is not possible, since Bessling et al. (1998) did not provide information about the feed mass flow and the distillate to feed ratio, which are key parameters for the design of reactive distillation processes. It also has to be considered that their process model does not account for the influence of the reaction kinetics, since they assume chemical equilibrium on all stages, as well as for the hydrodynamic behavior of the column internals. The model presented here considers the latter and therefore the reflux ratio is limited to values below 5, since otherwise flooding occurs.

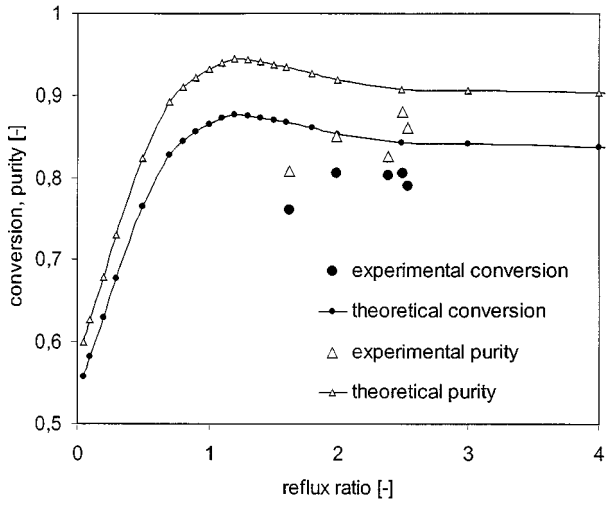

Figure 8. Theoretical vs. experimental results.

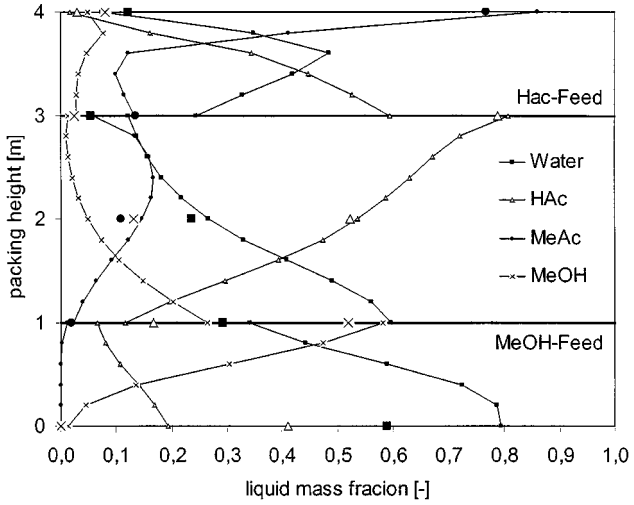

Figure 9. Liquid-phase composition profiles.

The experimental results do not confirm the simulated process behavior, since the experiments are limited to reflux ratios between 1 and 2.5. Thus, the strong decrease in conversion and purity towards lower reflux ratio could not be observed. The experimental conversion is 4 to 11% lower than the theoretical values, a phenomenon that can be explained with a reduced activity of the catalyst inside the column, but an extended data basis is needed to confirm this assumption. For the same reason, the experimental purity of the distillate is 3 to 12% lower than the theoretical values.

Figure 9 shows the composition of the liquid phase along the column height, with process conditions chosen according to experiment No. 6. The theoretical values are displayed with continuous lines, while the experimental results for the samples taken along the column lines are shown by single data points.

A maximum concentration of methanol and acetic-acid can be observed at the feed-locations respectively, while methyl acetate is enriched towards the top and water towards the bottom of the column. The experimental data show that the simulation results reflect the real process behavior of methyl acetate synthesis, but deviations between simulated and experimental composition profiles can still be observed.

Conclusions

The new type of catalytic packing MULTIPAK that shows a wide loading range combined with high separation efficiency and catalytic activity has been presented in this article. The main packing characteristics pressure drop and separation efficiency have been determined experimentally for the whole loading range and compared with data for conventional structured packings taken from literature. The pressure drop of MULTIPAK can be estimated with the hydraulic model of Rocha et al. (1996), but new models considering the special hydrodynamic behavior of catalytic packings are necessary to reflect the packing characteristics with good accuracy and to provide information about the scale-up behavior. A correlation for mass-transfer coefficients in both phases is presented that represents the experimental data with good accuracy.

Experiments have been performed in a pilot-scale reactive distillation column to investigate the behavior of a continuous process. A rigorous dynamic model based on the Maxwell-Stefan approach to describe mass transfer between phases has been modified and implemented in the simulation environment Aspen Custom Modeler. Steady-state simulations for the process of methyl-acetate synthesis have been performed and compared with experimental data. It was shown that the model is able to reflect the process behavior, but deviation was observed between experimental and theoretical conversion and purity. However, by implementing the reaction kinetics and the hydrodynamics of the catalytic packings in the process simulation, their influence on design aspects of reactive distillation columns were taken into account.

Acknowledgments

The support from Axiva GmbH, BASF AG, Bayer AG, Degussa-Hüls AG, and German Federal Ministry of Education and Research Project No. 03C0306 is highly appreciated.

Notation

a = specific packing surface, m^2/m^3
c = molar density, mol/m^3
d = column diameter, m
D = diffusivity, m^2/s
$\mathcal{D}$ = Maxwell-Stefan diffusivity, m^2/s
F = F-factor, $kg^{0.5}/m^{0.5}\cdot s$
(J) = vector of diffusion fluxes, $mol/m^2\cdot s$
$\dot{G}$ = gas mol flow, mol/s
h = specific enthalpy J/mol
h_L = volumetric holdup
H = height, m
HETP = height equivalent of a theoretical plate, m
HTU = height of transfer unit, m
k_{OG} = overall gas-phase mass-transfer coefficient m/s
K^{eq} = vapor liquid equilibrium constant
$\dot{L}$ = liquid mol flow, mol/s
m = stripping factor
$\dot{m}$ = mass flow, kg/h
n = number of components
$\dot{n}$ = interfacial molar flux, mol/m^2s
n_{th} = number of theoretical stages
NTSM = number of theoretical stages per meter, L/m
$\dot{q}$ = heat flux, $J/m^2\cdot s$
r = reaction rate, $mol/kg\cdot s$
$[R]$ = inverse mass-transfer coefficient matrix, s/m
Re = Reynolds number
S = corrugation side, m
Sc = Schmidt number
Sh = Sherwood number
T = temperature, K
u = velocity, m/s
w = mass fraction
x = liquid-phase mol fraction
y = gas-phase mol fraction
α = relative volatility
β = mass-transfer coefficient, m/s
$[\Gamma]$ = matrix of thermodynamic correction factors
δ = film thickness, m
ϵ = void fraction
η = viscosity, $Pa\cdot s$
θ = inclination angle
κ = individual mass-transfer coefficients, m/s
λ = thermal conductivity, $W/m\cdot K$
ρ = density, kg/m^3
ξ = conversion
ψ_{cat} = catalyst volume fraction
Δz = segment height, m

Subscripts

B = bottom
cat = catalyst
D = distillate
eff = effective
exp = experimental
F = feed
G = gas phase
i = component index
j = segment index
k = component index
L = liquid phase
s = superficial
t = total

Superscripts

av = average
ν = heat loss
$*$ = at the interface

Dimensionless numbers

Reynolds number = $Re_G = [(u_{G,eff} + u_{L,eff})\rho_G S]/\eta_G$
Schmidt number = $Sc_G = \eta_G/\rho_G D_G$
Sherwood number = $Sh_G = \beta_G S/D_G$

Literature Cited

Agreda, V. H., L. R. Partin, and W. H. Heise, "High-Purity Methyl Acetate via Reactive Distillation," *Chem. Eng. Prog.*, **86** (Feb. 1990).

Bart, H. J., and H. Landschützer, "Heterogene Reaktivdestillation mit axialer Rückvermischung," *Chem. Ing. Tech.*, **68**, 944 (1996)

Bessling, B., J. M. Löning, A. Ohligschläger, G. Schembecker, and K. Sundmacher, "Investigations on the Synthesis of Methyl Acetate in a Heterogeneous Reactive Distillation Process," *Chem. Eng. Technol.*, **21**, 393 (1998).

Chilton, T. H., and A. P. Colburn, "Distillation and Absorption in Packed Columns," *Ind. Eng. Chem.*, **27**, 255 (1935).

Ellenberger, J., and R. Krishna, "Counter-Current Operation of Structured Catalytically Packed Distillation Columns: Pressure Drop, Holdup and Mixing," *Chem. Eng. Sci.*, **54**, 1339 (1999).

Fair, J. R., "Design Aspects for Reactive Distillation," *Chem. Eng.*, 158 (Oct. 1998).

Frey, T., and J. Stichlmair, "Thermodynamic Fundamentals of Reactive Distillation," *Chem. Eng. Technol.*, **22**, 11 (1999).

Higler, A. P., R. Taylor, and R. Krishna, "Nonequilibrium Modelling of Reactive Distillation: Multiple States in MTBE Synthesis," *Chem. Eng. Sci.*, **54**, 1389 (1999).

Huang, C., G. G. Podrebarac, F. T. T. Ng, and G. L. Rempel, "A Study of Mass Transfer Behaviour in a Catalytic Distillation Col-

umn,'' *Can. J. Chem. Eng.*, **76**, 323 (1998).
Kenig, E., K. Jakobsson, P. Banik, J. Aittamaa, A. Górak, M. Koskinen, and P. Wettmann, ''An Integrated Tool for the Synthesis and Design of Reactive Distillation,'' *Chem. Eng. Sci.*, **54**, 1347 (1999).
Krafczyk, J., and J. Gmehling, ''Einsatz von Katalysatorpackungen für die Herstellung von Methylacetat durch reaktive Rektifikation,'' *Chem.-Ing. Tech.*, **66**, 1372 (1994).
Kreul, L. U., A. Górak, C. Dittrich and P. I. Barton, ''Dynamic Catalytic Distillation: Advanced Simulation and Experimental Validation,'' *Comp. Chem. Eng.*, **22**, Suppl., 371 (1998).
Krishna, R., and G. L. Standart, ''Mass and Energy Transfer in Multicomponent Systems,'' *Chem. Eng. Commun.*, **3**, 201 (1979).
Lee, J. H., and M. P. Dudukovic, ''A Comparison of the Equilibrium and Nonequilibrium Models for a Multicomponent Reactive Distillation Column,'' *Comp. Chem. Eng.*, **23**, 159 (1998).
Moritz, P., B. Bessling, and G. Schembecker, ''Fluiddynamische Betrachtungen von Katalysatorträgern bei der Reaktivdestillation,'' *Chem. Ing. Tech.*, **71**, 131 (1999).
Moritz, P., and H. Hasse, ''Fluid Dynamics in Reactive Distillation Packing Katapak-S,'' *Chem. Eng. Sci.*, **54**, 1367 (1999).
Nisoli, A., M. F. Malone. and M. F. Doherty, ''Attainable Regions for Reaction with Separation,'' *AIChE J.*, **43**, 374 (1997).
Offenlegungsschrift, Deutsches Patentamt, DE 197 01 045 A1, (1997).
Okasinski, M. J., and M. F. Doherty, ''Thermodynamic Behavior of Reactive Azeotropes,'' *AIChE J.*, **43**, 2227 (1997).
Olujić, Ž., A. B. Kamerbeek, and J. de Graauw, ''A Corrugation Geometry Based Model for Efficiency of Structured Distillation Packing,'' *Chem. Eng. Proc.*, **38**, 683 (1999).
Onken, U., and W. Arlt, ''Recommendet Test Mixtures for Distillation Columns,'' The Institution of Chemical Engineers, Warwickshire, U.K. (1990).
Pelkonen S., R. Kaesemann and A. Górak, ''Distillation Lines for Multicomponent Separation in Packed Columns—Theory and Comparison with Experiment,'' Ind.. Eng. Chem. Res, **36**, 5392 (1997).
Podrebarac, G. G., F. T. T. Ng, and G. L. Rempel, ''The Production of Diacetone Alcohol with Catalytic Distillation: I. Catalytic Distillation Experiments,'' *Chem. Eng. Sci.*, **53**, 1067 (1998a).
Podrebarac, G. G., F. T. T. Ng, and G. L. Rempel, ''The Production of Diacetone Alcohol with Catalytic Distillation: II. A Rate-Based Catalytic Distillation Model for the Reaction Zone,'' *Chem. Eng. Sci.*, **53**, 1077 (1998b).
Pöpken, T., R. Geisler, L. Götze, A. Brehm, P. Moritz, and J. Gmehling, ''Reaktionskinetik in der Reaktivrektifikation—Zur Übertragbarkeit von kinetischen Daten aus einer Rührzelle auf einen Rieselbettreaktor,'' *Chem.-Ing. Tech.*, **71**, 96 (1999).
Pöpken, T., L. Götze and J. Gmehling, ''Reaction Kinetics and Chemical Equilibrium of Homogeneously and Heterogeneously Catalyzed Acetic Acid Esterification with Methanol and Methyl Acetate Hydrolysis,'' *Ind. Eng. Chem. Res.*, **39**, 2601 (2000).
Powers, M. F., D. J. Vickery, A. Arehole, and R. Taylor, ''A Nonequilibrium Stage Model of Multicomponent Separation Processes: V. Computational Methods for Solving the Model Equations,'' *Comp. Chem. Engng.*, **12**, 1229 (1988).
Reid, R. C., J. M. Prausnitz, and B. E. Poling, *The Properties of Gases & Liquids*, 4th ed., McGraw Hill, New York (1987).
Rocha, J. A., J. L. Bravo and J. R. Fair, ''Distillation Columns Containing Structured Packings: A Comprehensive Model for Their Performance: 1. Hydraulic Models,'' *Ind. Eng. Chem. Res.*, **32**, 641 (1993).
Rocha, J. A., J. L. Bravo, and J. R. Fair, ''Distillation Columns Containing Structured Packings: A Comprehensive Model for Their Performance: 2. Mass-Transfer Model,'' *Ind. Eng. Chem. Res.*, **35**, 1660 (1996).
Schneider, R., C. Noeres, L. U. Kreul, and A. Górak, ''Dynamic Modelling and Simulation of Reactive Batch Distillation,'' *Comp. Chem. Engng.*, **23**, Suppl., 423 (1999).
Stichlmair, J. G., and J. R. Fair, *Distillation: Principles and Practice*, Wiley-VCH, New York, (1998).
Stewart, W. E., and R. Prober, ''Matrix Calculation of Multicomponent Mass Transfer in Isothermal Systems,'' *Ind. Eng. Chem. Fundam.*, **4**, 224 (1964).
Subwalla, H., and J. R. Fair, ''Design Guidelines for Solid-Catalyzed Reactive Distillation Systems,'' *Ind. Eng. Chem. Res.*, **38**, 3696 (1999).
Subwalla, H., J. C. Gonzalez, A. F. Seibert and J. R. Fair, ''Capacity and Efficiency of Reactive Distillation Bale Packing: Modelling and Experimental Validation,'' *Ind. Eng. Chem. Res.*, **36**, 3821 (1997).
Sundmacher, K., and U. Hoffman, ''Development of a New Catalytic Distillation Process for Fuel Ethers via a Detailed Nonequilibrium Model,'' *Chem. Eng. Sci.*, **51**, 2359 (1996).
Taylor, R., and R. Krishna, *Multicomponent Mass Transfer*, Wiley, New York (1993).
Taylor, R., and R. Krishna, ''Modelling Reactive Distillation,'' *Chem. Eng. Sci.*, **55**, 5183 (2000).
Ung, S., and M. F. Doherty, ''Necessary and Sufficient Conditions for Reactive Azeotropes in Multireaction Mixtures,'' *AIChE J.*, **41**, 2383 (1995).
Xu, Z. P., and K. T. Chuang, ''Kinetics of Acetic Acid Esterification over Ion Exchange Catalysts,'' *Can. J. Chem. Eng.*, **74**, 493 (1996).
Xu, Z. P. and K. T. Chuang, ''Effect of Internal Diffusion on Heterogeneous Catalytic Esterification of Acetic Acid,'' *Chem. Eng. Sci.*, **52**, 3011 (1997).
Xu X., Z. Zhao, and S. Tian, ''Study on Catalytic Distillation Processes: III: Prediction of Pressure Drop and Holdup in Catalyst Bed,'' *Trans IChemE*, **75**, 625 (1997).
Zheng, Y., and X. Xu, ''Study on Catalytic Distillation Processes: Part I. Mass Transfer Characteristics in Catalyst Bed within the Column,'' *Trans IChemE*, **70**, 459 (1992).

Manuscript received Jan. 18, 2000, and revision received Feb. 12, 2001.